THE SPRING RESEARCH AND MANUFACTURERS' ASSOCIATION

FATIGUE FAILURES OF LIGHT SPRINGS

Final Report

ON THE REASONS FOR SCATTER OF FATIGUE RESULTS OBTAINED FOR COMPRESSION SPRINGS MADE FROM BS5216 ND3 WIRE

Report No. 358

by

L. F. Reynolds, M.Sc.Tech., C.Eng., M.I.M.

MAY 1983

THE SPRING RESEARCH AND MANUFACTURERS' ASSOCIATION

FATIGUE FAILURES OF LIGHT SPRINGS

Final Report

ON THE REASONS FOR SCATTER OF FATIGUE RESULTS OBTAINED FOR COMPRESSION SPRINGS MADE FROM BS5216 ND3 WIRE

Report No. 358

by

L. F. Reynolds, M.Sc.Tech., C.Eng., M.I.M.

SUMMARY

Fatigue tests have been carried out on compression springs made from 2.65 mm BS5216 ND3 wire obtained from two sources of supply. Previous work at S.R.A.M.A. had indicated that, for springs made from the wires, the scatter of fatigue results was greater for one of the wires than for the other.

A combination of optical microscopy and scanning electron fractography was used both to characterize the fatigue fractures and to determine the reasons for early failures which were observed.

The work has demonstrated that partial decarburization to a depth of only 0.025 mm (representing 0.9% of the wire diameter) induced a small number of fatigue failures at lifes an order of magnitude lower than those expected for wire which was free from decarburization.

It is suggested that shot peening the springs will eliminate such early failures, but that futher investigation is required to identify the defect levels below which such early failures can be avoided.

CONTENTS

9. Spring A36: Sample re-oriented to show shear fracture and tensile fracture more clearly
10. Spring A36: Detail of shear/tensile fracture transition zone
11. Spring A36: Detail of shear/tensile fracture transition zone
12. Spring A56: 9.37×10^6 cycles: General appearance of fracture initiation, close to inside of spring coil
13. Spring A56: Fracture initiation in more detail.
14. Spring A56: Detail of longitudinal shear initiation and transition to 45° tensile
15. Spring C35: 1.2×10^6 cycles: General appearance of fracture initiation close to inside of spring coil
16. Spring C35: Fracture initiation in more detail
17. Spring C35: Sample re-oriented to show shear fracture and tensile fracture more clearly
18. Spring C35: Detail of shear/tensile fracture transition zone
19. Spring C35: Detail of shear/tensile fracture transition zone
20. Spring C59: 7.2×10^6 cycles: General appearance of fracture initiation close to inside of spring coil
21. Spring C59: Fracture initiation in more detail
22. Spring C59: Sample re-oriented to show shear fracture and tensile fracture more clearly
23. Spring C59: Detail of shear/tensile fracture transition zone
24. Spring C59: Detail of shear/tensile fracture transition zone
25. Spring A83: 1.62×10^5 cycles (early failure due to salt corrosion): General appearance of fracture initiation due to corrosion, close to inside of spring coil
26. Spring A83: Fracture initiation in more detail
27. Spring A83: More detail of fracture initiation. Note absence of longitudinal shear (Stage I) crack
28. Spring A83: Detail of fracture initiation confirming that failure commenced in 45° tensile mode (Stage II) at the spring surface
29. Spring C36: 2.2×10^5 cycles (early failure due to partial

decarburization): General appearance of fracture initiation close to inside of spring coil

30. Spring C36: Fracture initiation in more detail
31. Spring C36: Sample re-oriented to show shear fracture and tensile fracture more clearly
32. Spring C36: Detail of one of shear/tensile transition zones
33. Spring C36: Optical photomicrograph of longitudinal shear (Stage I) fatigue crack initiated at region of partial decarburization

FATIGUE FAILURES OF LIGHT SPRINGS
Final Report
ON THE REASONS FOR SCATTER OF FATIGUE RESULTS OBTAINED FOR COMPRESSION SPRINGS MADE FROM BS5216 ND3 WIRE

1. INTRODUCTION

A previous S.R.A.M.A. report presented fatigue data generated at an initial stress of 1OON/mm^2, for compression springs made from 2.65 mm diameter BS5216 ND3 wire which was obtained from four suppliers, identified as A, B, C and D[1].

The work confirmed that all four wires fully conformed to the requirements of BS5216. 1975 for ND3 wire.

Wires A, B and D showed no evidence of decarburization or surface defects, but wire C exhibited partial decarburization up to 0.9% of the wire diameter, which was within the 1.5% of the nominal wire diameter permitted by BS5216 for this material.

Springs made from wires A and C were selected for more detailed examination in the present work, since they represented the extremes of surface quality, in respect of partial decarburization, and fatigue scatter.

In particular, springs made from wire C tended to give fatigue lifes which were generally lower than those exhibited by the other three wires, whilst simultaneously displaying a tendency to increased scatter. Similar observations were made in previous work at S.R.A.M.A., which showed that the fatigue ratio of hardened and tempered carbon steel springs, made from 2.8 mm wire, was reduced from 0.52 to 0.46 when partial decarburization was present in the surface to a depth of 0.025 mm[2].

2. EXPERIMENTAL TECHNIQUES

2.1 Mechanical Properties of Wire

The mechanical properties of the wires were reported in the earlier work at S.R.A.M.A.[1].

The appropriate information concerning the tensile and torsional properties of wires A and C after heat treatment at 250°C/½ hour are given in Tables I and II for the present work.

2.2 Spring Design and Fatigue Testing

Full details of the spring design and the fatigue testing technique were given in the previous S.R.A.M.A. report[1]. The nominal spring design is shown in Table III however. For each of the wires A and C, 20 springs were fatigue tested from an initial stress of 100N/mm^2 to maximum stresses of 750N/mm^2, which was close to the fatigue limit of the springs, and 1000N/mm^2 respectively. When added to the 4 springs similarly tested at each of these stresses during the previous work, it was intended that a total of 24 fatigue tested springs should be made available from each wire batch for detailed analysis and examination, thus representing the behaviour of springs made from each wire at each level of maximum stress. In the event, the number of broken springs per batch available for detailed analysis varied from 18 to 24, due to unavoidable losses as a result of 1 corrosion failure, 6 run-outs at 10^7 cycles and 2 springs which broke at an undetermined life, having incapacitated the machine cut-off mechanism upon failure.

2.3 Examination of Wire Surfaces and Spring Fractures

All the broken springs were examined using a stereoscopic optical microscope, to determine the general fracture characteristics displayed by the fatigue failures.

The Cambridge Instruments S4 scanning electron microscope (SEM) at the S.R.A.M.A. Laboratories was employed to examine in detail both the surface of the wire used to make the springs, and the fracture characteristics of selected springs which failed at a maximum stress of 750N/mm^2.

SEM examination of the wire surfaces was carried out after the wire samples had been cleaned to remove surface contamination, using a combined chemical and ultrasonic cleaning technique, the details of which have been presented in an earlier S.R.A.M.A. report[3].

The spring fractures selected for electron microscopy were ultrasonically cleaned in trichlorethylene immediately prior to examination on the SEM.

2.4 Optical Microscopy of Broken Springs

Transverse microsections were prepared for selected springs from wire batches A and C. After etching in 2% Nital, the polished samples were examined for evidence of partial decarburization and surface defects.

2.5 Further Investigation of Springs A83 and C36

Springs A83 and C36, tested at a fatigue stress range of 100-750N/mm^2, gave comparatively short lives and, in addition to the SEM examination, further investigation was necessary to establish the precise causes of failure.

Several transverse microsections were prepared for both these springs, for detailed examination on the optical metallurgical microscope.

In the event optical microscopy suggested a reason for the early failure of spring C36, but gave no indications as to the reason for failure of spring A83 and hence more intensive investigation of this spring was required. With the co-operation of the Metallurgy Department of Sheffield University, the fracture surface of spring A83 was examined by means of a Phillips PSEM500 Scanning Electron Microscope which was equipped with an Electon Energy Dispersive Analyser. This combination of equipment was capable of both indentifying the features characterising the fracture, and of simultaneously providing qualitative anaylses of selected areas, approximately 1µm in diameter, for chemical elements with atomic numbers above, and including, that of sodium (Atomic No. = 11). This

technique suggested a possible reason for the observed early failure of spring A83.

3. RESULTS AND DISCUSSION

3.1 Mechanical Properties of Wires

Statistical analysis of the mechanical property results indicated that Wire A tended to exhibit tensile and torsional properties which were higher than those of Wire C, the difference in the appropriate mean values being significant at the 98% level, and higher, of the 't' distribution.

In general, there was no difference in the scatter of the tensile properties. Statistical analysis suggested that there may have been a difference in the scatter of the torsional limit of proportionality for the two wires, the variance of Wire C being significantly higher than that of Wire A at the 95% level of the 'F' distribution. More samples would be required, however, to test the propriety of this finding.

3.2 Scanning Electron Microscopy of Wire Surfaces

The results of SEM examination are shown in Figs. 4 and 5 for Wire A and Wire C respectively. The wire surfaces were typical of those previously observed at S.R.A.M.A. for very similar material, and detailed investigations have shown that the apparent differences in surface roughness do not exert a significant influence on the fatigue performance of springs made from the wires[3].

3.3 Optical Microscopy of Broken Springs

Optical microscopy of the springs confirmed the findings published in an earlier report with respect to surface defects and partial decarburization[1].

Thus springs from wire batches A and C were essentially free from surface defects. Furthermore, springs of Batch A showed no evidence of partial decarburization.

By contrast, the springs of Batch C exhibited intermittent partial decarburization around 70-80% of the wire circumference, to maximum depths of 0.025 mm representing approximately 0.9% of the wire diameter.

3.4 Fatigue Properties and Fracture Characteristics of Springs

3.4.1 Stress Range 100-1000N/mm^2

The fatigue results for springs tested within this stress range are shown plotted in Fig. 1, from which it is apparent that there were no significant differences in the mean fatigue lifes of springs made from Wires A and C. By contrast, the variance of the Batch C springs was approximately 2½-3 times greater than that obtained for the Batch A springs, and Snedecor's 'F' test indicated that the difference in scatter of fatigue results was significant at the 99% level of the 'F' distribution. This result is substantiated by consideration of the range of fatigue results obtained for the two spring batches as shown below:-

Wire Batch	Range of Fatigue Life, Cycles*	
	Minimum	Maximum
A	1.29×10^5 (A75)	3.87×10^5 (A72)
C	5.76×10^4 (C16)	3.38×10^5 (C63)

* Figures in parantheses are spring identification numbers, retained for ease of reference at S.R.A.M.A.

These data confirm that the scatter of Batch C springs was substantially greater than that of Batch A springs.

Examination of all the spring fractures on a stereoscopic optical microscope revealed no major differences in fracture appearance for the components made from Wires A and C. Almost without exception, the fatigue cracks initiated in the 45^{o} direction of maximum tensile stress, from the inside regions of the first active coil. For each batch of springs, about 70% of the fractures initiated at tooling marks, but the fatigue life and scatter of such failures were not significantly different from those of the failures associated with the more usual features of fatigue crack initiation and propogation in the absence of tooling marks. Initiation of fatigue cracks was therefore relatively easy in these springs tested within the stress range 100-1000N/mm^2, and growth of the microscopic Stage II tensile crack occupied a significant proportion of the total fatigue life.

3.4.2 Stress Range 100-750N/mm^2

The fatigue results for springs tested within this stress range are shown plotted in Fig. 2.

After omission of spring A83 (which failed prematurely to the influence of corrosion and is considered later in more detail), there was no statistically significant difference in either the mean life or the variance of the broken springs made from wires A and C.

Nevertheless, consideration of the results shown in Fig. 2 reveals that there was a significant difference in the range of fatigue lifes exhibited by the two batches of springs, as indicated in the following table:

Wire Batch	Range of Fatigue Life, Cycles*	
	Minimum	Maximum
A	1.61×10^6 (A36)	9.37×10^6 (A56)
C	2.21×10^5 (C36)	7.24×10^6 (C59)

* Figures in parantheses are spring identification numbers, retained for ease of reference at S.R.A.M.A.

Furthermore, the range shown for springs made from Wire Batch C was a conservative estimate, since 6 of the 24 springs tested remained unbroken after 10^7 cycles (implying that the fatigue limit of the Batch C springs may have been higher than that of the Batch A springs), whilst 2 springs failed at lifes of less than 10^6 cycles.

Optical examination of all the springs on a stereoscopic binocular microscope showed that, almost without exception, spring failure was initiated on the inside of the first active coil, but at a position approximately 20 degrees around the circumference, from the inside coil location usually assumed to experience the maximum shear stress.

With the exception of spring A83, all the fractures showed similar characteristics under optical examination. Initiation of the fatigue crack was associated with a small, sometimes barely discernible, zone of longitudinal shear. The growing fatigue crack subsequently transformed into a smooth zone of propagation in the 45° plane of maximum resolved tensile stress, which finally led to a region of fast overload fracture culminating in complete failure of the component. This general mode of torsional fatigue failure has been described in an earlier S.R.A.M.A. report [4].

Spring A83 was unusual in that fracture initiation had apparently occurred at more than one point of the inside coil region, with little evidence of longitudinal shear at the initiation zones.

No significant differences in fracture characteristics were apparent during optical examination of springs made from Wires A and C, however, and hence more detailed examination of representative fractures was carried out using the Scanning Electron Microscope.

The following samples were selected as being suitable for SEM examination of the fatigue fractures.
(See also Fig. 2):-

SEM SAMPLES

Spring Identification	Life Cycles	Reason for Examination on SEM
A36	1.61×10^6	Represents bottom of fatigue range for Batch A
A56	9.37×10^6	Represents top of fatigue range for Batch A
C35	1.2×10^6	Represents bottom of fatigue range for Batch C (approximately equivalent to spring A36)
C59	7.24×10^6	Represents top of fatigue range for Batch C
A83	1.62×10^5	Investigation of poor fatigue life
C36	2.21×10^5	Investigation of poor fatigue life

Scanning electron fractographs depicting the fatigue fractures of springs A36, A56, C35 and C59 are presented in Figs. 6-24, whilst those for springs A83 and C36 are shown in Figs. 25-28 and 29-32 respectively.

From the scanning electron fractographs, it was apparent that propagation of the fatigue crack generally occurred in two clearly identifiable stages, which can be catergorized as follows:-

1. Stage I Propagation: this mode of propagation generally entailed deepening of the initiated microcrack in the direction of maximum longitudinal shear stress.

2. Stage II Propagation: in this region, the fatigue crack propagated in the 45° plane of maximum tensile stress, leading to a final fast fracture which culminated in complete failure of the spring.

The transfer from Stage I (longitudinal shear) to Stage II (45° tensile) crack propagation generally occurred at a region 20-125 μm, below the spring surface.

There was no significant relationship, however, between fatigue performance and the depth of the Stage I - Stage II transition zone, as can be seen from the data plotted in Fig. 3, thus implying that initiation of a microcrack and/or subsequent shear (Stage I) propagation was intrinsically more difficult for some samples than for others. The reason for this difference in behaviour is not yet clear.

The findings with respect to the early failures observed for springs A83 and C36 were particularly revealing, however.

Spring A83 (1.62×10^5 cycles)

Examination on the SEM showed that Stage I (shear) crack propagation was completely absent in this spring, the fatigue crack having proceeded directly into the Stage II (45° tensile) mode of propagation from the inside surface of the coil (see Fig. 28).

Optical microscopy revealed no evidence of surface defects or decarburization which might have adversely affected the fatigue life of the spring.

A more detailed examination of the fracture surface was carried out using a Scanning Electron Microscope with an analytical attachment. This examination indicated that both sodium and chlorine were present at regions of the spring surface associated with the crack origin, thus suggesting that the short fatigue life was associated with saline (NaCl) contamination at the spring surface.

The source of the original contamination was not clearly established, however. Nevertheless, this result was particularly interesting in that the Stage II fracture surface of spring A83 was very similar in character to those observed for the remaining five springs examined on the SEM.

In general terms, these observations may indicate that complete failure of all springs occurred about 2×10^5 cycles after the transition into Stage II crack propagation. Thus crack initiation, and Stage I growth

into a shear microcrack approximately 20-100 μm in length, apparently occupied more than 95% of the total fatigue life for springs with a mean survival of approximately 4 x 10^6 cycles. Similar observations have been made in the past for fatigue of smooth ductile materials at relatively low applied stresses [5].

Spring C36 (2.21 x 10^5 cycles)

Scanning electron microscopy clearly established that both Stage I and Stage II regions of crack propagation were involved in fatigue failure of this spring (see Fig. 31).

In this respect, therefore, fracture of spring C36 did not differ substantially from that of spring C59, for example, which survived for 7.24 x 10^6 cycles before failure (see Fig. 22).

In consequence, the results of the SEM examination did not explain the early failure of spring C36.

Transverse microsections from a region just behind the fracture face were prepared for examination on the optical microscope.

After etching in 2% Nital, it became apparent that partial decarburization was present to a depth of 0.025 mm at the regions of the spring associated with the fatigue crack origin. Furthermore, several examples were observed of longitudinal shear (Stage I) fatigue cracks propagating along the ferrite "spines" at these areas of partial decarburization (see Fig. 33).

The effective torsional elastic limit of a compression spring is given by the solid stress of the component, i.e. approximately 1400N/mm^2 for the present spring design, after stress relieving and pre-stressing. By contrast, the torsional elastic limit of the pure ferrite region of decarburization is of the order of 100-120N/mm^2, and hence the ferrite "spines" would be significantly overstressed at the applied maximum stress of 750N/mm^2 which was employed for the fatigue tests.

Consequently crack initiation and Stage I (shear) crack propagation probably occurred relatively quickly in spring C36, leading to early transition into Stage II (tensile) propagation and subsequent rapid failure of the spring.

The fact that this spring experienced early failure as a direct result of surface decarburization indicates that this aspect of the fatigue behaviour must be considered an intrinsic feature of the fatigue properties of springs containing the observed levels of partial decarburization.

This finding suggests that some early fatigue failures may be expected to occur in unpeened springs made from BS5216 ND3 wire containing levels of decarburization lying well within the 1½% of the nominal wire diameter permitted by the specification. Under these circumstances, it may be necessary to shotpeen springs made from spring steel wire where partial decarburization may be present, so as to avoid such early failures. Previous work has demonstrated that shot peening is an effective method of reducing the incidence of early fatigue failures of springs, even when significant amounts of partial decarburization are present in the spring surface [6,7,8].

4. CONCLUSIONS

1. Although Wire A exhibited both tensile and torsional properties which were significantly higher than those of Wire C, there was no difference of any statistical significance in the mean fatigue lifes of springs made from the Wires when tested at stresses of both 100-1000N/mm^2 and 100-750N/mm^2.

2. The scatter, and in particular the range, of fatigue lifes associated with springs made from Wire C, which exhibited partial decarburization to a depth of 0.025 mm, was consistently greater than that observed for springs made from Wire A, which was completely free of decarburization.

3. Optical microscopy has shown that partial decarburization to a maximum depth of 0.025 mm can induce premature fatigue failures even at a relatively low value of maximum stress, which was close to the fatigue limit of the springs, with a possibility of springs breaking at lifes an order of magnitude less than the mean fatigue life of the springs.

4. A combination of optical and scanning electron microscopy of the fatigue fracture surfaces obtained for springs broken at a maximum stress of $750N/mm^2$, has shown that, in the absence of external influences such as corrosion, fatigue cracks initiated in longitudinal shear at the inside regions of the first active coil, but at a position approximately 20° removed, around the circumference, from the inside coil zone of maximum applied stress.

5. The work indicated that at a maximum stress of $750N/mm^2$, and in the absence of premature failure as a result of partial decarburization, over 95% of the fatigue life was spent in initiation of the fatigue crack, and subsequent propagation in longitudinal shear (Stage I crack propagation) to a crack depth of 25-120 μm.

6. At a depth of 25-120 μm in the longitudinal shear (Stage I) crack transferred into tensile propagation in the 45° direction of maximum tensile stress (Stage II) and complete failure of the springs followed shortly afterwards, within approximately 2×10^5 cycles. There was no apparent relationship between the depth of the Stage I→ Stage II transition and the fatigue life, however.

7. One spring (A83) failed prematurely as a result of saline contamination at the wire surface. Scanning electron microscopy showed that this type of failure was characterized by a complete absence of longitudinal shear (Stage I) propagation, fracture having initiated directly into the 45° tensile mode of propagation (Stage II) which led to rapid failure of the spring.

5. RECOMMENDATIONS

The work has indicated that partial decarburization to a depth of 0.025 mm can significantly influence the scatter of fatigue results, as exemplified by the range, for unpeened BS5216 ND3 springs made from 2.65 mm wire. Further work should be carried out to determine the levels of decarburization at which the effects upon scatter become significant. In particular, the effects of both wire size and decarburization levels upon the fatigue scatter of springs should be investigated, since salvaging of decarburized springs by effective shot peening is likely to prove difficult due to spring distortion at wire sizes less than about 1.2 mm.

6. REFERENCES

1. Reynolds, L.F., "Fatigue Failures of Light Springs, First Progress Report: Preliminary Examination of BS5216 ND3 Wires and the Fatigue Properties of Associated Compression Springs".
S.R.A.M.A. Report No. 351, April 1982.

2. Hood, A.R., "The Effect of Decarburization on the Fatigue Properties of Hardened and Tempered Carbon Steel Springs".
S.R.A.M.A. Report No. 329, June 1980.

3. Reynolds, L.F., "The Influence of Surface Roughness of as Drawn Wire upon the Fatigue Performance of Helical Compression Springs".
S.R.A.M.A. Report No. 298, October 1978.

4. Brummit, K., "On the Development of Failure During the Fatigue Testing of Torsion Bars".
S.R.A.M.A. Report No. 320, January 1980.

5. Duggan, T.V. and Byrne, J., "Fatigue as a Design Criterion", MacMillan Press, 1977. Chapter 4.

6. Watkinson, J., "The Fatigue Strength of Decarburized Steel Surfaces".
Coil Spring Journal, 35, June 1954. Pps. 14-42.

7. Kaiser, B., "The Influence of Decarburization and Surface Cold Working on Fatigue Strength". Wire, 32 (4) 1982, Pps. 223-228.

8. Kaiser, B., and Kosters, R., "Shot Peening Improves Fatigue Resistance of Springs".
Wire World International, 24 September/October 1982, Pps. 166-170.

TABLE I

TENSILE PROPERTIES OF WIRES AFTER L.T.H.T. 250°C./½ HOUR

Statistical Function	Tensile Properties, N/mm^2							
	Wire A				Wire C			
	Rm	L. of P.	$Rp_{0.05}$	$Rp_{0.1}$	Rm	L. of P.	$Rp_{0.05}$	$Rp_{0.1}$
Mean Value	1961	1267	1684	1792	1827	1332	1658	1730
Standard Deviation	4	140	26	14	5	98	19	12
No. of Tests	4	4	4	4	5	5	5	5

TABLE II

TORSIONAL PROPERTIES OF WIRES AFTER L.T.H.T. 250°C./½ HOUR

Statistical Function	Torsional Properties, N/mm^2							
	Wire A				Wire C			
	L. of P.	0.1% Proof Stress	0.2% Proof Stress	Modulus G	L. of P.	0.1% Proof Stress	0.2% Proof Stress	Modulus G
Mean Value	852	1058	1116	7.78×10^4	736	1007	1068	7.96×10^4
Standard Deviation	24	17	15	2.8×10^2	74	32	24	5.1×10^2
No. of Tests	5	5	5	5	5	5	5	5

TABLE III SPRING DESIGN

Wire Diameter	2.65 mm
Mean Coil Diameter	21.7 mm
Total Coils	5.5
Active Coils	3.5
Free Length*	43 mm
Solid Stress	1400N/mm^2

* After L.T.H.T. 250^{o}C./½ hour, prestressing and end grinding.

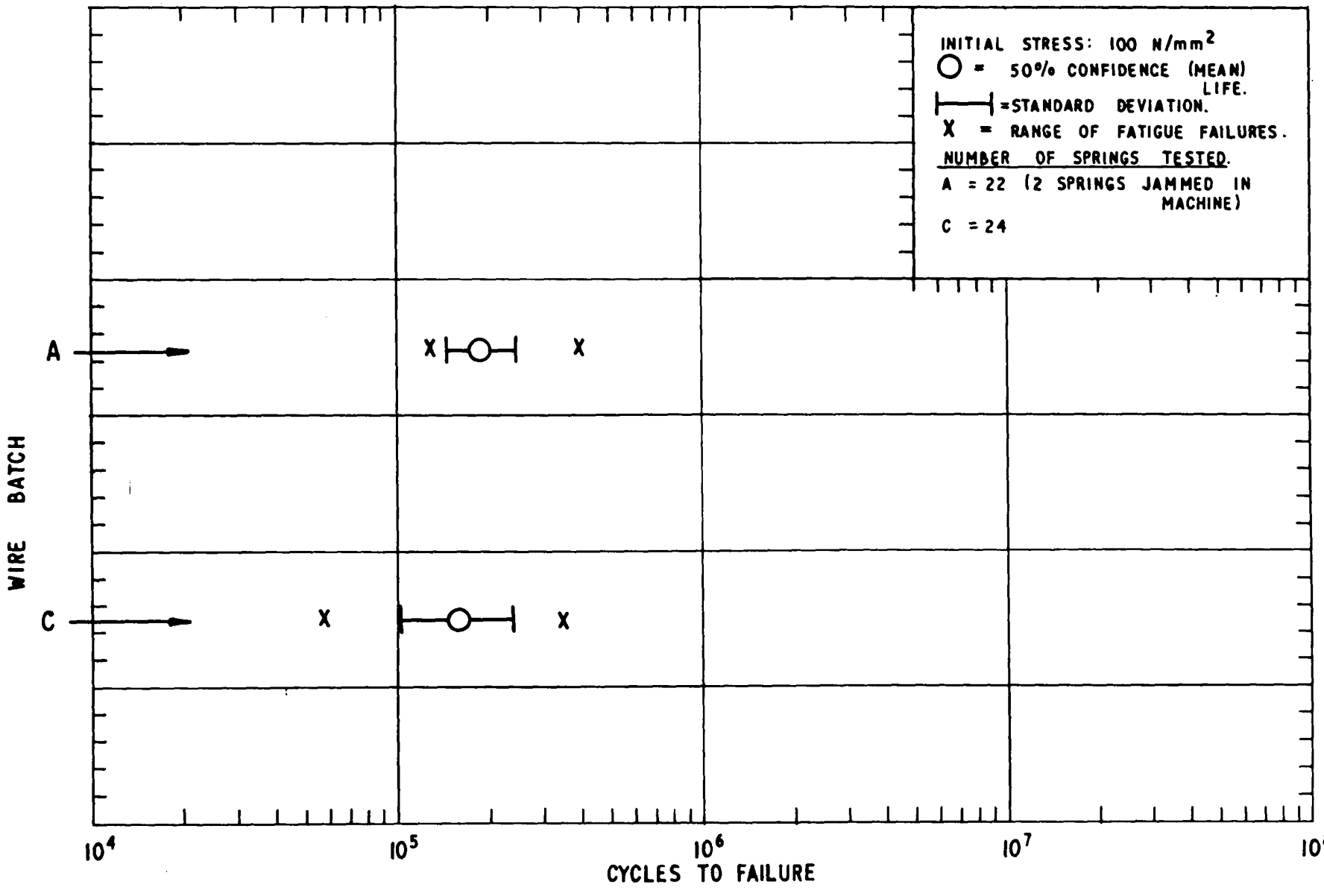

FIG. 1 FATIGUE OF BS 5216 ND 3 COMPRESSION SPRINGS: MAXIMUM STRESS 1000 N/mm²

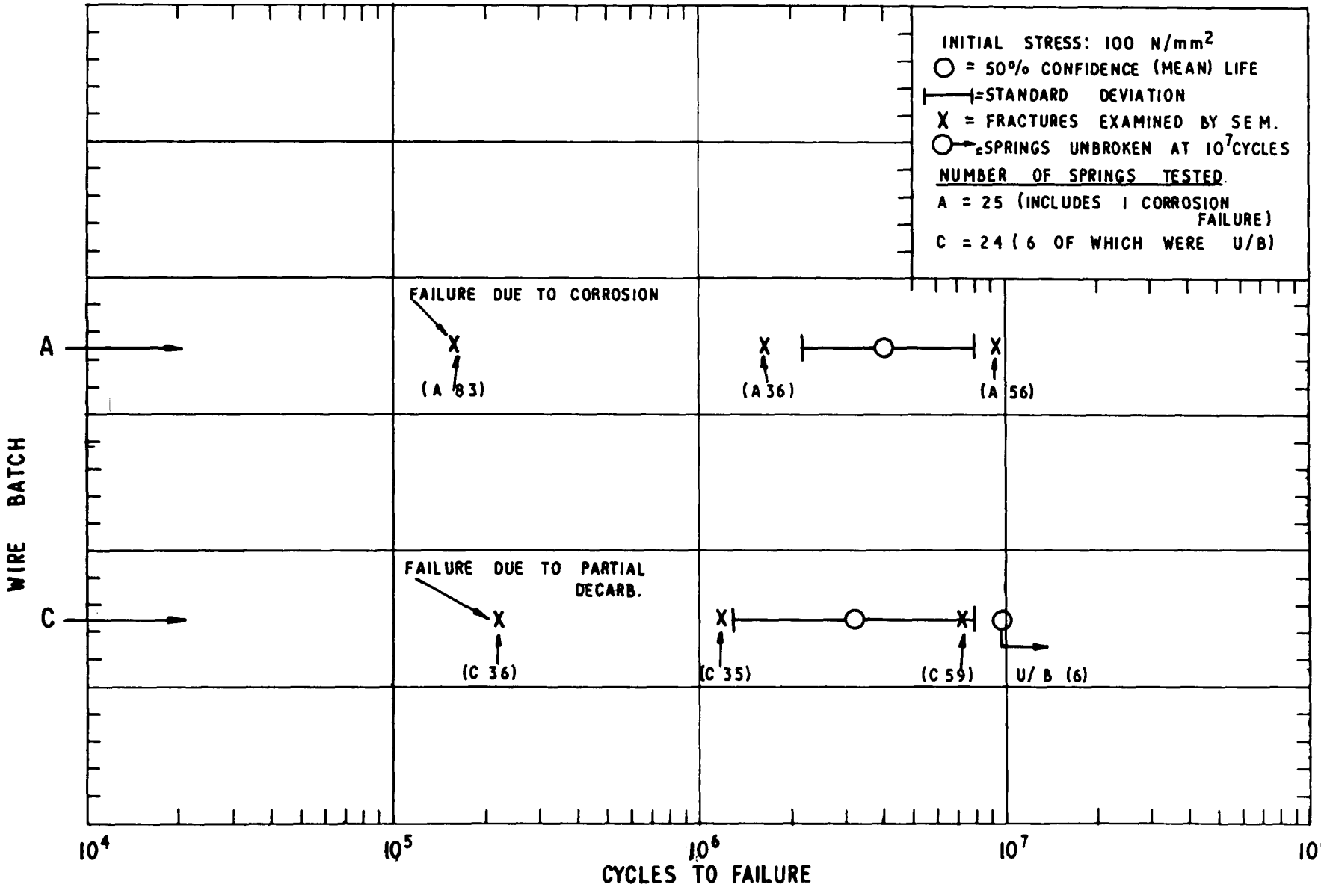

FIG. 2. FATIGUE OF BS 5216 ND3 COMPRESSION SPRINGS: MAXIMUM STRESS 750 N/mm²

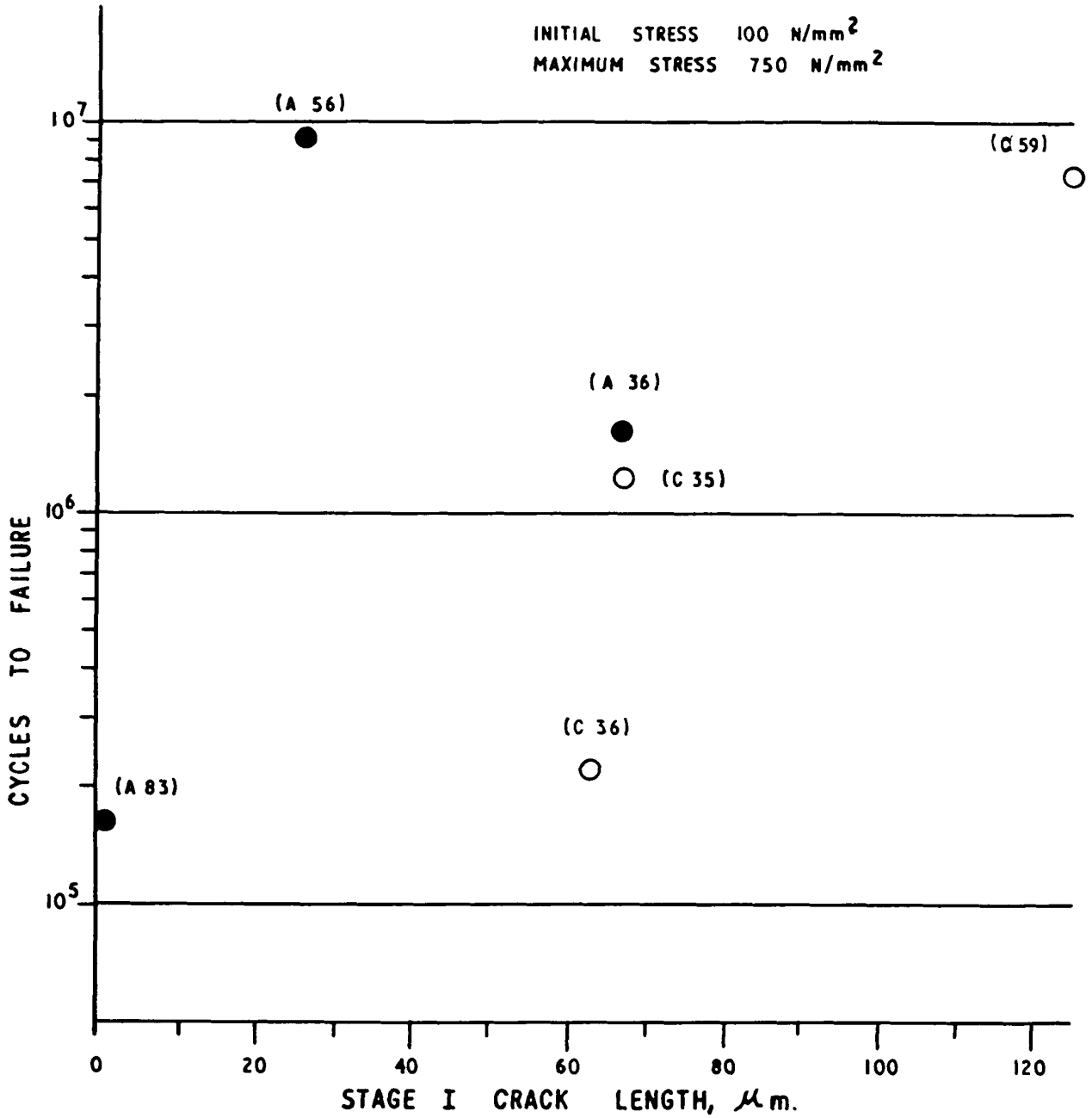

FIG. 3 FATIGUE LIFE OF SPRINGS PLOTTED AS A FUNCTION OF STAGE I (SHEAR) CRACK LENGTH.

APPEARANCE OF 2.65 mm BS5216ND3 WIRE SURFACE ON SCANNING ELECTRON MICROSCOPE

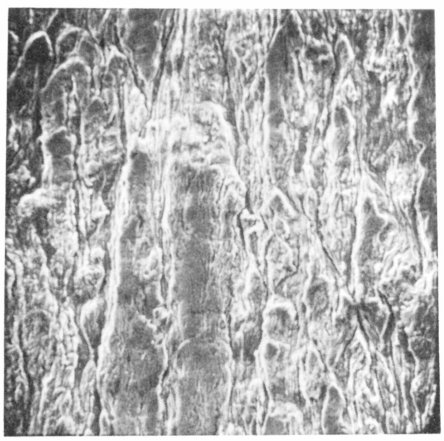

Fig 4 x 340

Wire A

Fig 5 x 340

Wire C

SCANNING ELECTRON FRACTOGRAPHY

SPRING A36; 1.61 x 10^6 CYCLES

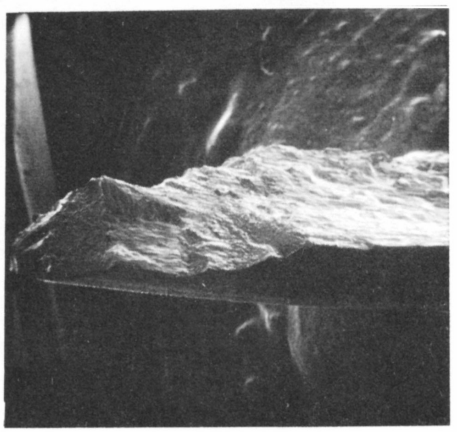

Fig 6 x 15

General appearance of fracture initiation, close to inside of spring coil

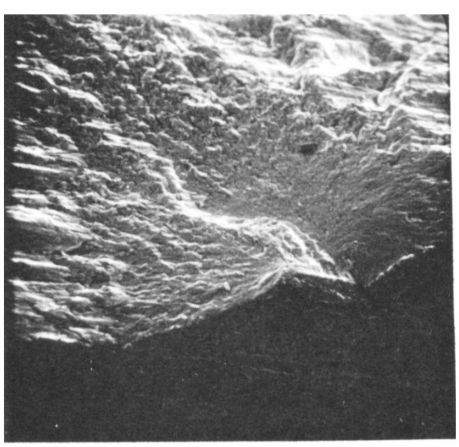

Fig 7 x 75

Fracture initiation in more detail

SPRING A36

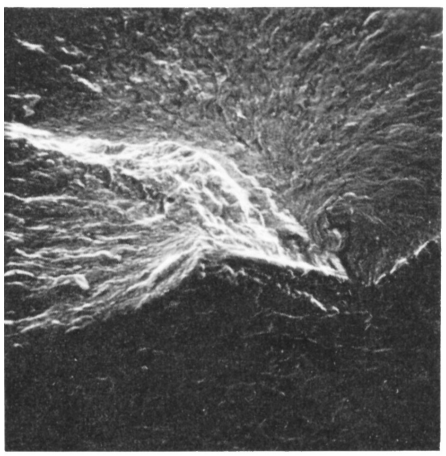

Fig 8 x 150
Detail of initiation at longitudinal shear step, (Stage I crack) and subsequent tensile fracture (Stage II crack)

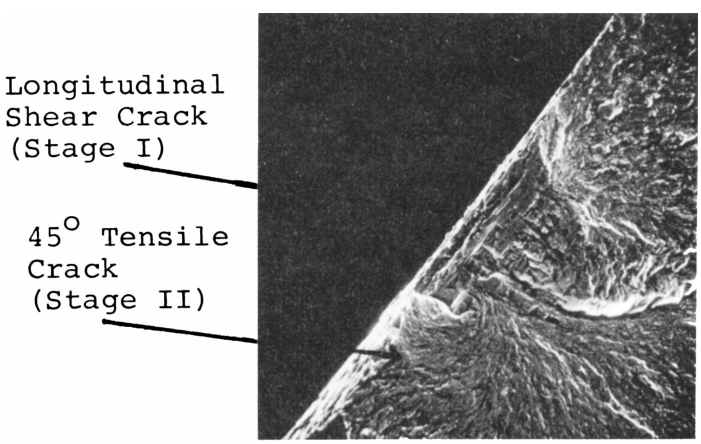

Fig 9 x 120
Sample re-oriented to show shear fracture and tensile fracture more clearly

SPRING A36

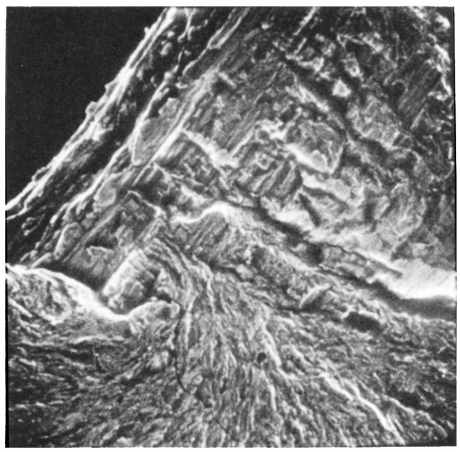

Fig 10 x 306

Detail of shear/tensile fracture transition zone

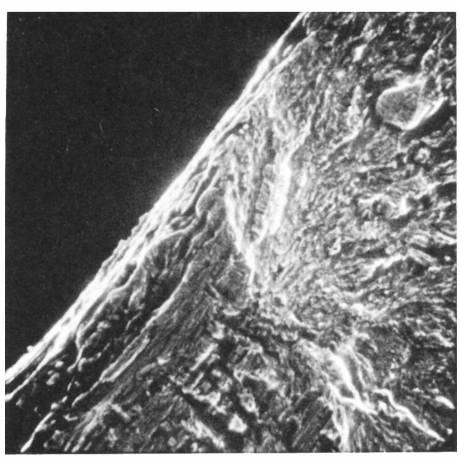

Fig 11 x 320

Detail of shear/tensile fracture transition zone

SCANNING ELECTRON FRACTOGRAPHY,

SPRING A56; 9.37 x 10^6 CYCLES

Fig 12 x 17

General appearance of fracture initiation, close to inside of spring coil

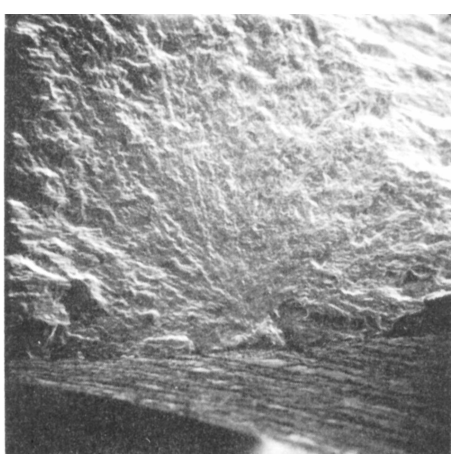

Fig 13 x 85

Fracture initiation in more detail

Fig 14 x 420

Detail of longitudinal shear initiation and transition to 45^o tensile

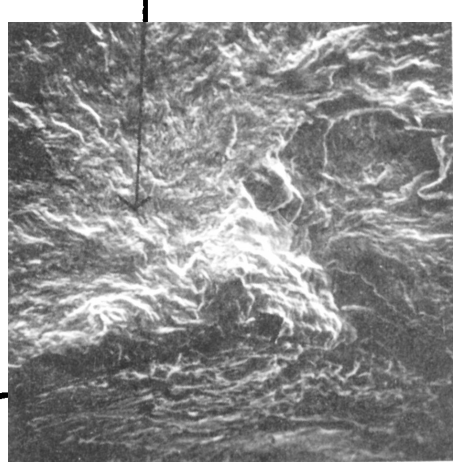

SCANNING ELECTRON FRACTOGRAPH

SPRING C35; 1.2 x 10^6 CYCLES

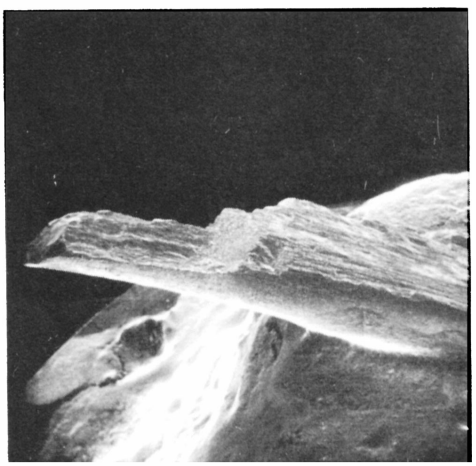

Fig 15 x 12

General appearance of fracture initiation close to inside of spring coil

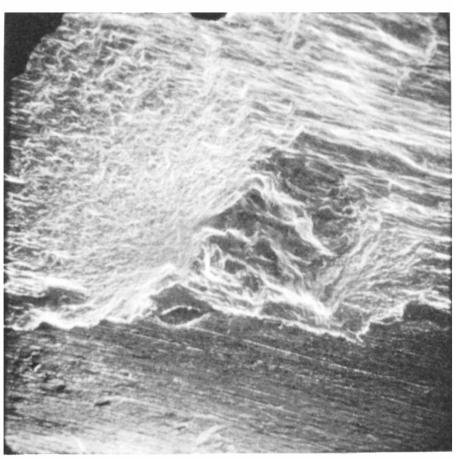

Fig 16 x 60

Fracture initiation in more detail

SPRING C35

Fig 17 x 17

Sample re-oriented to show shear fracture and tensile fracture more clearly

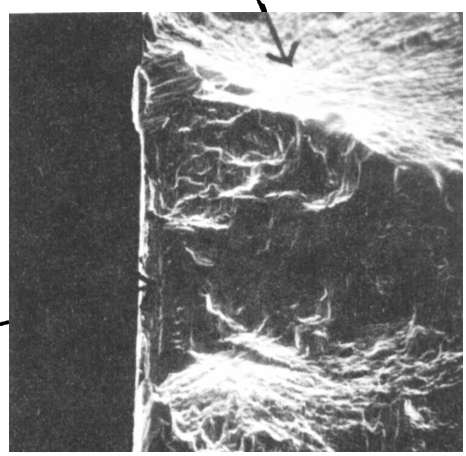

Fig 18 x 300

Detail of shear/tensile fracture transition zone

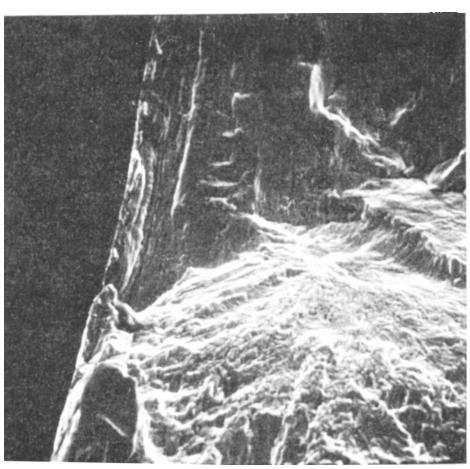

Fig 19 x 290

Detail of shear/tensile fracture transition zone

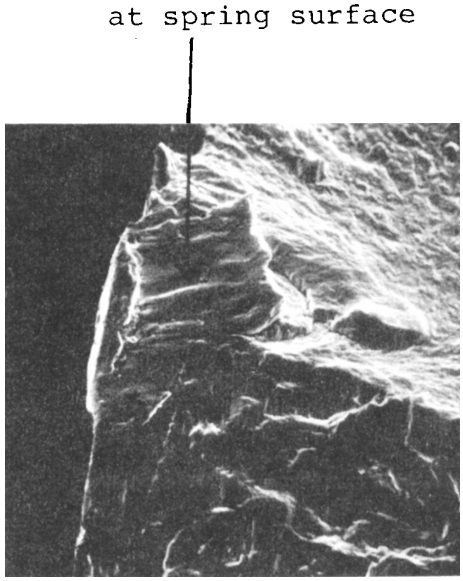

SCANNING ELECTRON FRACTOGRAPH

SPRING C59; 7.2 x 10^6 CYCLES

Fig 20 x 13

General appearance of fracture initiation close to inside of spring coil

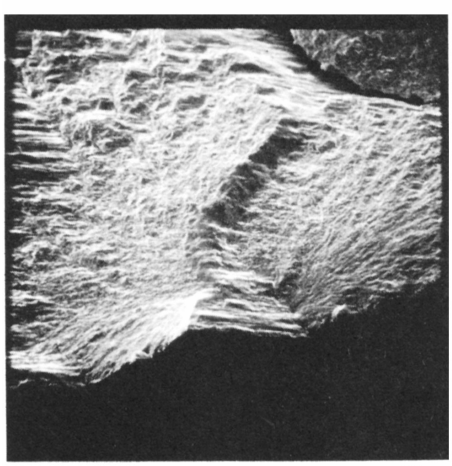

Fig 21 x 65

Fracture initiation in more detail

SPRING C59

Fig 22 x 120

Sample re-oriented to show shear fracture and tensile fracture more clearly

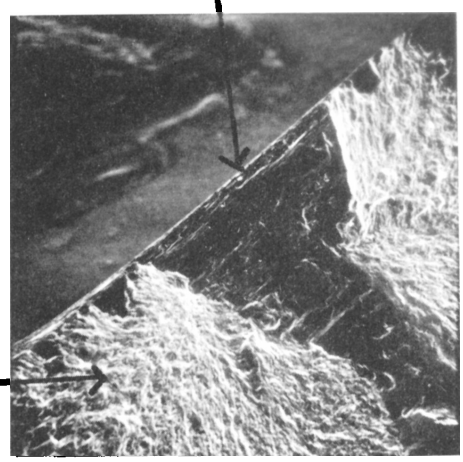

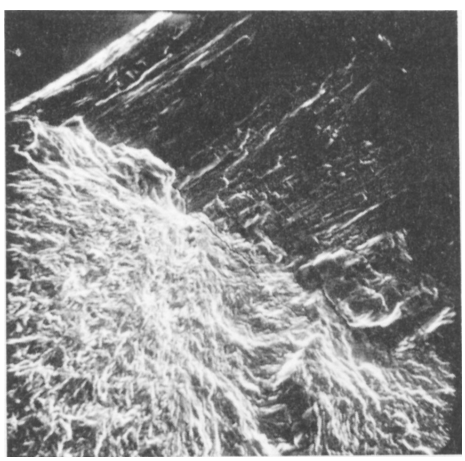

Fig 23 x 300

Detail of shear/tensile fracture transition zone

Fig 24 x 300

Detail of shear/tensile fracture transition zone

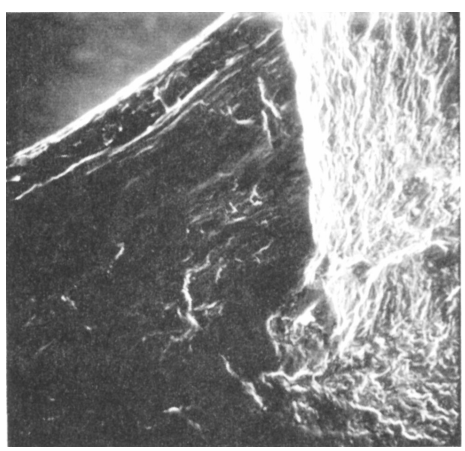

SCANNING ELECTRON FRACTOGRAPHY

SPRING A83; 1.62 x 10^5 CYCLES

(Early failure due to salt corrosion)

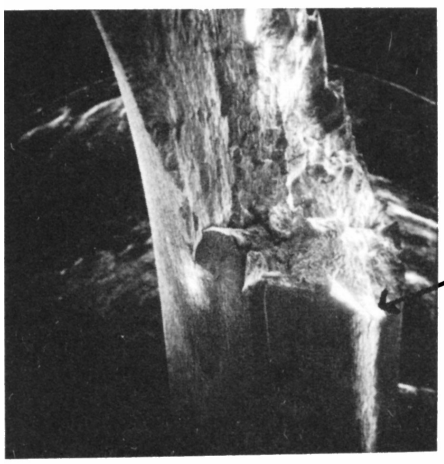

Fig 25 x 14

General appearance of fracture initiation due to corrosion, close to inside of spring coil

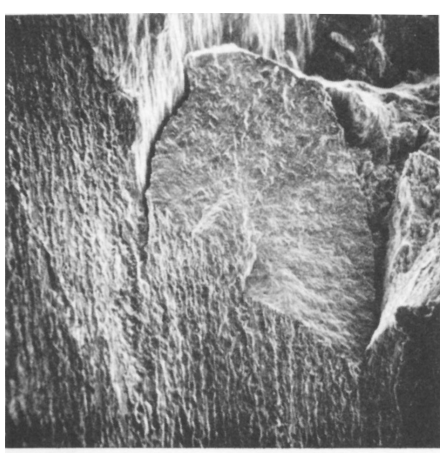

Fig 26 x 70

Fracture initiation in more detail

SPRING A83

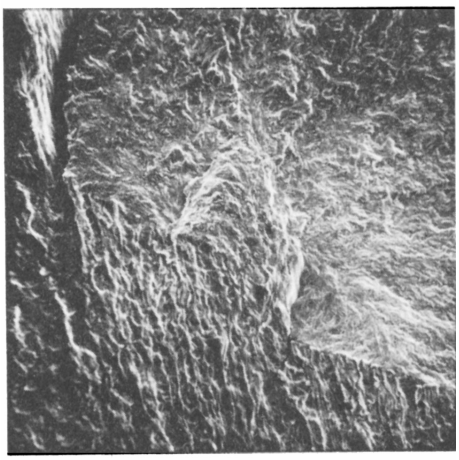

Fig 27 x 140
More detail of fracture initiation. Note absence of longitudinal shear (Stage I) crack

Fig 28 x 690
Detail of fracture initiation confirming that failure commenced in 45° tensile mode (Stage II) at the spring surface

SCANNING ELECTRON FRACTOGRAPHY

SPRING C36; 2.2 x 10^5 CYCLES

(Early failure due to partial decarburization)

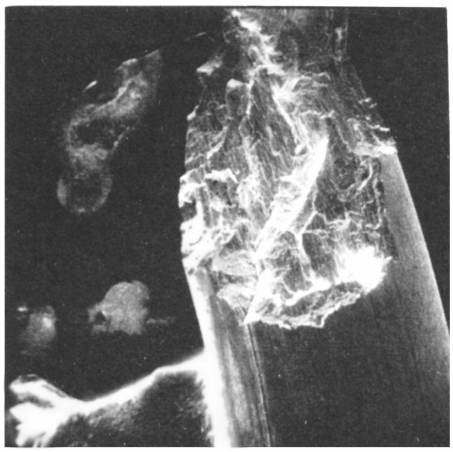

Fig 29 x 13

General appearance of fracture initiation close to inside of spring coil.

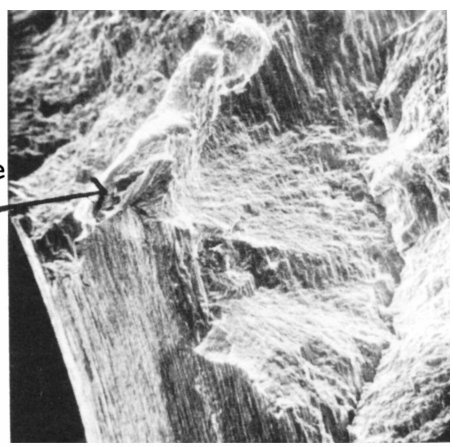

Fig 30 x 65

Fracture initiation in more detail.

SPRING C36

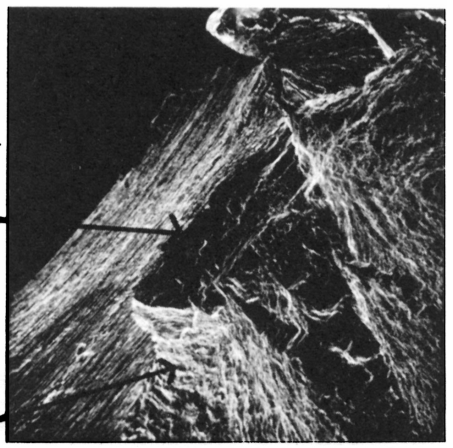

Fig 31 x 120

Sample re-oriented to show shear fracture and tensile fracture more clearly.

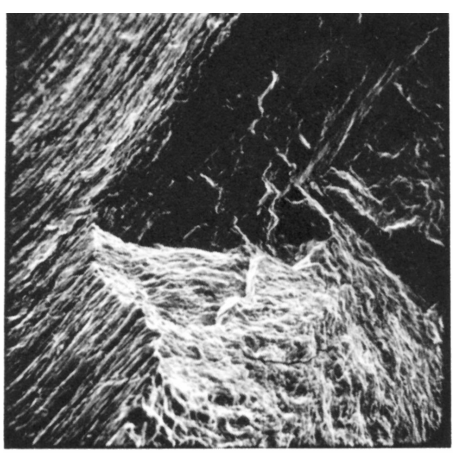

Fig 32 x 300

Detail of one of shear/ tensile transition zones. (Other transition zone was damaged during fatigue failure).

OPTICAL PHOTOMICROGRAPH

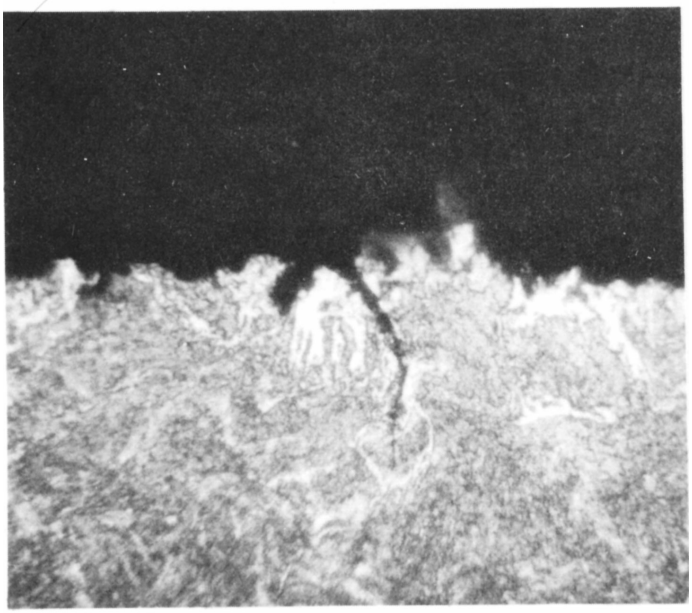

Fig 33 x 1060

Longitudinal shear (Stage I) fatigue crack initiated at region of partial decarburization in spring C36, which experienced early failure at 2.2×10^5 cycles.